Umklapp Electron-Phonon Scattering in the Low-Temperature Resistivity of Polyvalent Metals*

W. E. Lawrence

Department of Physics, Dartmouth College, Hanover, New Hampshire 03755

and

J. W. Wilkins

Laboratory of Atomic and Solid State Physics, Cornell University, Ithaca, New York 14850

(Received 20 July 1972)

A study of the effect of umklapp electron-phonon scattering on the low-temperature resistivity in polyvalent metals yields the following results: (i) The exponential $[\exp(-\Theta/T)]$ behavior in the alkalis is replaced by power laws in temperature; (ii) for single-OPW scattering states (i.e., spherical Fermi surface) a T^2 law results if a constant matrix element is used; if the wave-vector dependence of the matrix element in the vicinity of Bragg planes is included, a comparable T^4 law occurs; (iii) two-OPW corrections are important qualitatively only at the lowest temperatures, where they reduce the umklapp contribution to resistivity, distorting the power laws and producing the ultimate low-temperature behavior T^5. Nevertheless, the umklapp process strongly dominates the normal at all temperatures. The use of a simple trial function in the variational formula for resistivity makes the calculation and these results applicable to the temperature-dependent resistivity of impure metals. Comparison with experiment supports this interpretation.

I. INTRODUCTION

Our considerations of umklapp electron-phonon scattering are motivated by the observation that a T^5 power law does not dominate the low-temperature electrical resistivity in certain simple metals[1]. For example, Garland and Bowers[1] have analyzed such measurements in indium in terms of T^2 and T^5 components over a wide range of purities, and find a significant "T^2 component" in each case studied. In the case of aluminum, Ekin[2] has found similar deviations from the T^5 power law, but it appears impossible to assign a unique power law to the deviations. In aluminum alloys, and at somewhat higher temperatures (greater than about $\frac{1}{30}$th the Debye temperature), Caplin and Rizutto[3] have observed an approximate T^3 dependence in resistivity. Some of the experimental results are plotted in Figs. 1(a) and 1(b), along with our results for electron-phonon scattering. In each of these experiments, the temperature-dependent resistivity has a marked dependence on impurity resistivity.

The present authors[4] have investigated theoretically the contribution to resistivity from electron-electron scattering (originally suggested by Garland and Bowers because it is known to produce a T^2 dependence) and have concluded that it should be as great for the alkali metals Na and K as for the simple polyvalent metals Al and In. Since no T^2 term is observed experimentally in alkali metals, we are led instead to consider umklapp electron-phonon scattering as a source for the observed deviations from the T^5 law at low temperatures.

As the details of the calculations are fairly complicated and only approximate, it is perhaps useful to set out several aspects of the problem which will not be so obvious once we are in the midst of it. First, a brief review of the variational principle leading to a formula for the resistivity will be given. Then the effects of Fermi-surface geometry on the various parts of the resistivity formula will be analyzed to predict their contribution at low temperature. Finally we shall show how the resistivity formula can lead to an understanding of deviations from Matthiessen's rule.

A. Resistivity Formula (Variational)

We wish very briefly to review the derivation of the (Kohler) variational result for electrical resistivity in a notation appropriate to our uses. More detailed treatments are available elsewhere[5]. The Boltzmann equation for the electron distribution function $f(\vec{k})$ in the presence of a (unit) electric field $\hat{E}$ is

$$X(\vec{k}) \equiv \frac{\partial f^0(\vec{k})}{\partial E(\vec{k})} \, \vec{v}(\vec{k}) \cdot \hat{E} e$$

$$= -\sum_{\vec{k}'} P(\vec{k}, \vec{k}') [\Psi(\vec{k}) - \Psi(\vec{k}')], \qquad (1.1)$$

where the electron of charge e, energy $E(\vec{k})$, and velocity $\vec{v}(\vec{k})$ has an equilibrium distribution function $f^0(\vec{k})$. The deviation (from equilibrium) function $\Psi(\vec{k})$ can be thought of as the shift of single-particle energies due to the applied field:

$$f(\vec{k}) \approx f^0(\vec{k}) + \frac{\partial f^0(\vec{k})}{\partial E(\vec{k})} \Psi(\vec{k})$$

$$\simeq f^0(E(\vec{k}) + \Psi(\vec{k})) \; . \tag{1.2}$$

Finally the collision operator $P(\vec{k}, \vec{k}')$ which strives

to relax the nonequilibrium distribution can be written for the case of electron-phonon scattering as

$$P(\vec{k}, \vec{k}') = \frac{2\pi}{\hbar k_B T} \sum_\lambda |g_\lambda(\vec{k}, \vec{k}')|^2 \; \frac{f^0(\vec{k}) f^0(\vec{k}')}{|e^{-E(\vec{k})/k_B T} - e^{-E(\vec{k}')/k_B T}|} \; [\delta(E(\vec{k}) - E(\vec{k}') - \hbar\omega_{q\lambda}) + \delta(E(\vec{k}) - E(\vec{k}') + \hbar\omega_{q\lambda})] \; . \tag{1.3}$$

Note that (1.3) is invariant to the interchange of $\vec{k}$ and $\vec{k}'$. In this section we work in the extended zone scheme (in the course of the detailed calculations the reduced zone scheme will be more convenient). Hence the division into normal and umklapp processes is simple:

Normal: $\vec{k} - \vec{k}'$ in first Brillouin zone ;

Umklapp: $\vec{k} - \vec{k}'$ not in first Brillouin zone . $\tag{1.4}$

In either case the phonon wave vector q always lies in the first Brillouin zone so that

$$\vec{k} - \vec{k}' = \vec{q} + \vec{G} \; , \tag{1.5}$$

where $\vec{G}$ is a reciprocal-lattice vector. Then the matrix element $g_\lambda(\vec{k}, \vec{k}')$ for the scattering of an electron from $\vec{k}$ to $\vec{k}'$ through the emission or absorption of a phonon with wave vector $\vec{q}$, polarization $\hat{\epsilon}_{q\lambda}$, and energy $\omega_{q\lambda}$ is

$$|g_\lambda(\vec{k}, \vec{k}')|^2 = (\hbar/MN\omega_{q\lambda}) |m_\lambda(\vec{k}, \vec{k}')|^2 \; , \tag{1.6}$$

where

$$m_\lambda(\vec{k}, \vec{k}') = \langle \vec{k} | \hat{\epsilon}_{q\lambda} \cdot \vec{\nabla} V | \vec{k}' \rangle \tag{1.7}$$

is the reduced matrix element, N is the density of unity cells, and M the ionic mass.

With this unavoidable detail out of the way, we return to (1.1) which we observe can be written, dropping the arguments, as

$$X = H \Psi \; , \tag{1.8}$$

where H is a real, symmetric integral operator. The conductivity can likewise be written in a similar simple fashion

$$\sigma = \sum_{\vec{k}} e\vec{v}(\vec{k}) \cdot \hat{E} \; \frac{\partial f^0}{\partial E(\vec{k})} \; \Psi(\vec{k})$$

$$= \sum_{\vec{k}} \Psi(\vec{k}) X(\vec{k}) = (\Psi, X) \; , \tag{1.9}$$

where the convention in the second line of (1.9) is (hopefully) obvious. Let Ψ_t be some trial function which is reasonably well behaved; then the Schwarz inequality gives

$$(\Psi_t, H\Psi_t)(\Psi, H\Psi) \geq (\Psi_t, H\Psi)^2 \; . \tag{1.10}$$

The application of (1.8) and (1.9) to (1.10) gives an upper bound on the resistivity[6]

$$\rho = \sigma^{-1} \leq (\Psi_t, H\Psi_t)/(\Psi_t, X)^2 \; . \tag{1.11}$$

This form will be useful for general discussions later, but a more explicit form is immediately needed. The standard trial function is

$$\Psi_0(\vec{k}) = \vec{v}(\vec{k}) \cdot \hat{E} \; , \tag{1.12}$$

where only the *angular* dependence of $\vec{v}(\vec{k})$ on the Fermi surface is retained. Each sum over $\vec{k}$ can be written as a product of an integral over $E(k)$ and one over the Fermi surface S_k. Then we find that

$$\rho \leq \frac{\pi}{6\hbar} \left(\frac{1}{4\pi^3\hbar}\right)^2 \int \frac{dS_k}{|\vec{v}(\vec{k})|} \; \frac{dS_{k'}}{|\vec{v}(\vec{k})|} \left(\; |\vec{v}(\vec{k}) - \vec{v}(\vec{k}')|^2 \right.$$

$$\left. \times \sum_\lambda |g_\lambda(\vec{k}, \vec{k}')|^2 f(\hbar\omega_{q\lambda}/k_B T) \right) \Big/ (\Psi_t, X)^2 \; . \tag{1.13}$$

We have not bothered to write out (Ψ_t, X) since it does not contribute to the temperature dependence of the resistivity. The factor $f(\hbar\omega/k_B T)$ results from the integral over the energy variables and is given by

$$f(x) = x/[(e^x - 1)(1 - e^{-x})] \; . \tag{1.14}$$

The only important points about $f(\hbar\omega/k_B T)$ are (i) that it falls off exponentially for finite x and (ii) that it is the source of *all* the temperature dependence of ρ, as we shall see.

Finally we should observe that the velocity-transfer term

$$\tfrac{1}{2} |\vec{v}(\vec{k}) - \vec{v}(\vec{k}')|^2$$

comes from observing that inside the integrals it is equal to

$$\vec{v}(\vec{k}) \cdot (\vec{v}(\vec{k}) - \vec{v}(\vec{k}')).$$

The symmetric form is clearly more convenient for complicated geometries. For the case where $\vec{v}(\vec{k})$ is proportional and parallel to $\vec{k}$, either expression reduces to the well known $(1 - \hat{k} \cdot \hat{k}') = 1 - \cos\theta$.

B. Temperature Dependence of ρ due to Normal and Umklapp Processes

In order to extract the low-temperature behavior of the resistivity we must determine the small-q (hence small ω_q) dependence of the three factors comprising (1.13):
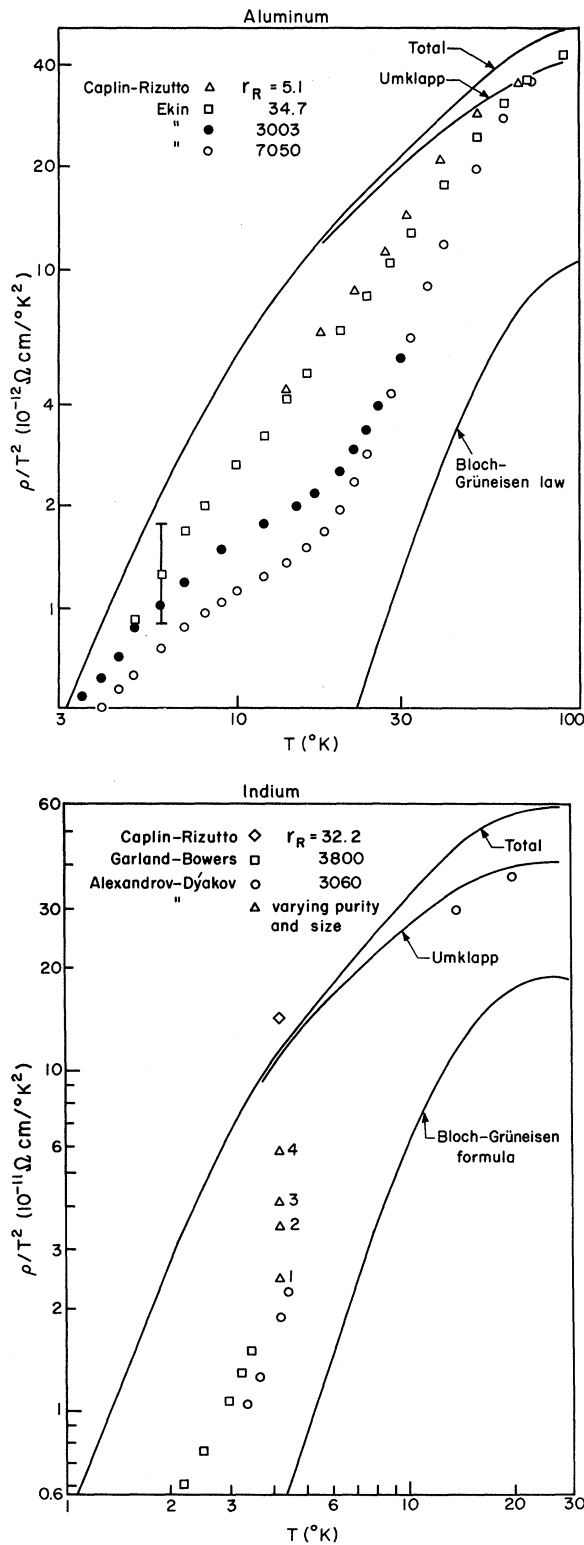
FIG. 1. Measurements on samples of various purity compared with the results of this work (upper curves) and with the Bloch–Grüneisen formula (lower curve). The same Debye temperature, corresponding to the transverse phonon modes, is used in both curves.

(i) phase-space integral: $\int dS_k \, dS_{k'}$,   (1.15a)

(ii) velocity transfer: $\left| \vec{v}(\vec{k}) - \vec{v}(\vec{k'}) \right|^2$,   (1.15b)

(iii) (matrix element)^2: $\left| g_\lambda(\vec{k}, \vec{k'}) \right|^2$.   (1.15c)

If the resultant q dependence is $q^n dq$, then ρ is proportional to T^{n+1}, due to the homogeneity of $f(\hbar\omega/k_B T)$.

That the temperature dependence due to normal and umklapp processes will be different seems obvious if only because $\vec{v}(\vec{k}) - \vec{v}(\vec{k'})$ will "surely" be different in the two cases. That the same umklapp process may produce a different temperature dependence at different temperatures is less obvious. The important point is that the distortion of the Fermi surface due to the band gap $V(G)$ determines a characteristic wave vector $q \sim k_F(V(G)/E_F)$ and hence a characteristic temperature.

$$\Theta_1 \sim \Theta_D(V(G)/E_F) ,   (1.16)$$

where Θ_D is the Debye temperature. Since $V(G)/E_F$ of the order of 0.01 to 0.05 are common, it is possible that for $\Theta_1 < T \ll \Theta_D$ the distortions of the Fermi surfaces would *not* be important in the resistivity while for $T < \Theta_1$ they would. These two regimes give different temperature dependences. We will illustrate this by considering each of three factors (1.15a)–(1.15c) in turn.

1. Phase-Space Factor

Our aim is to write (1.15a) as an integral over q:

$$\int dS_k \, dS_{k'} = \int dq \, P(q) ,   (1.17)$$

where presumably $P(q)$ can be expressed as a power series in q. Consider first a *normal* scattering event. In that case both the initial and final electron wave vectors $\vec{k}$ and $\vec{k'}$, lie on the same Fermi sphere, as shown in the extended-reduced zone spheres of Fig. 2(a). The phase space $P_N(q) \, dq$ for such an event is the number of pairs of points $(\vec{k}, \vec{k'})$ on the sphere whose separation $|\vec{k'} - \vec{k}|$ is within dq of q. For given initial state $\vec{k}$ the number of appropriately distant final states is $2\pi q \, dq$. The number of initial states is simply the Fermi-surface area $4\pi k_F^2$, so the total number of pairs is

$$P_N(q) \, dq = 8\pi k_F^2 q \, dq \sim q \, dq   (1.18)$$

which is recorded in Table I.

Turning now to the umklapp process, consider first the case where $T > \Theta_1$, so that any distortion of the Fermi surface from a sphere can be ignored. Then referring to Fig. 2(b), an umklapp scattering event is one in which $\vec{k}$ and $\vec{k'}$ lie on different spheres in the reduced zone scheme. For a scattering event with reduced momentum transfer $\vec{q}$ to
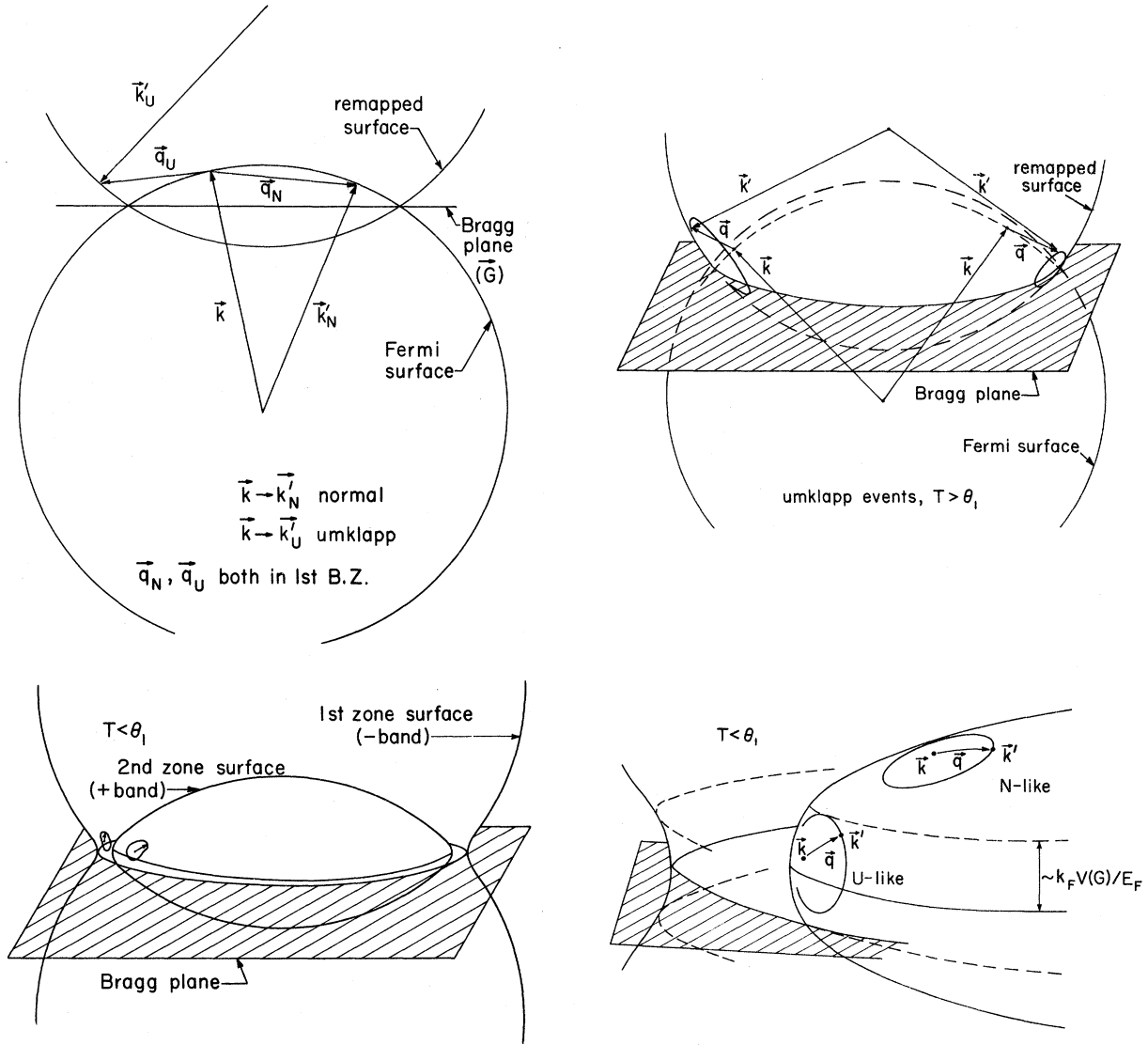
FIG. 2. (a) Normal and umklapp events. (b) Umklapp events with fixed q. (c) and (d) Scattering through small q on a distorted surface.

occur at all, the initial state must lie within a distance q of the second, or remapped, sphere. The locus of such initial states is a strip centered about each of the Bragg planes ($\pm \vec{G}$). The area of each strip is $4\pi q k_F^2/G$. For a given initial state $\vec{k}$ in one of these strips, the number of appropriately distant final states is $2\pi q \, dq$. So the umklapp scattering phase space, taking the contribution from each of the two strips, is

$$P_U(q)\, dq = (16\pi^2 k_F^2/G)\, q^2\, dq \sim q^2\, dq \ .$$

In other words, an additional factor of q appears in $P_U(q)$ because both $\vec{k}$ and $\vec{k}'$ must lie within a distance q from the intersection of the two spheres in order for an umklapp process to occur.

TABLE I. The q dependences of three factors in the resistivity integrand determine the temperature dependences from normal scattering, and from umklapp scattering in the two temperature regimes. Momentum dependence of the form factor adds an umklapp contribution proportional to T^4 for $T > \Theta_1$, and to T^5 for $T < \Theta_1$.

| | | Umklapp | |
Kind of process	Normal	$T > \Theta_1$	$T < \Theta_1$
Phase space	$q\,dq$	$q^2\,dq$	$q\,dq$
Velocity transfer	q^2	G^2	q^2
(Matrix element)^2	q	$1/q$	q
Total integrand	$q^4\,dq$	$q\,dq$	$q^4\,dq$
Temperature dependence	T^5	T^2	T^5

Finally consider the case $T < \Theta_1$, where distortions in the Fermi surface are important [see Figs. 2(c) and 2(d)]. Since

$$|\vec{k}' - \vec{k}| < [V(G)/E_F]k_F ,$$

and furthermore since both wave vectors must lie within that distance from the Brillouin-zone plane, the surface *available* for scattering is roughly a *flattish cylinder*. Accordingly, as in the normal scattering case, the number of appropriately distant (from $\vec{k}$) final states is $2\pi q\, dq$, and the number of initial states is independent of q, $\sim 2\pi k_F [k_F V(G)/E_F]$. The net result is that at low temperatures $(T < \Theta_1)$, we again recover the phase-space factor $q\, dq$ as for normal processes.

2. Velocity-Transfer Factor

The discussion of the velocity-transfer factor

$$|\vec{v}(\vec{k}) - \vec{v}(\vec{k}')|^2 \qquad (1.15b)$$

is considerably simpler. For a spherical Fermi surface $\vec{v}(\vec{k}) \sim \vec{k}$. Since $|\vec{k}' - \vec{k}| = q$ for a normal process, $(1.15b) \sim q^2$. In the case of umklapp processes where we may neglect the Fermi-surface distortions $(T > \Theta_1)$, $|\vec{k}' - \vec{k}| = |\vec{G} + \vec{q}|$. Accordingly $(1.15b) \sim G^2$. Finally at very low temperatures $(T < \Theta_1)$ the distortion of the Fermi surface destroys any direct connection between $\vec{v}$ and $\vec{k}$. But clearly on the lens-shaped surface in Figs. 2(c) and 2(d), the velocity is continuous across the Bragg plane. Not suprisingly, a direct calculation in Sec. III gives $(1.15b) \sim q^2$, again. All of these results are recorded in Table I.

3. (Matrix Element)^2

To discuss the matrix element we note since $\omega_q \propto q$ for small q, that from (1.6) and (1.7),

$$|g_\lambda(\vec{k}, \vec{k}')|^2 \propto |\langle \vec{k}| \hat{\epsilon}_{q\lambda} \cdot \vec{\nabla} V|\vec{k}'\rangle|^2/q . \qquad (1.19)$$

The fourier transform of V (above) has no singular dependence and is a constant at small q. Any interesting behavior arises from the gradient in (1.19). For normal processes and for umklapp ones where $T > \Theta_1$, the states $\vec{k}$ and $\vec{k}'$ may be represented by plane waves. Accordingly, the gradient produces $\vec{q}$ and $\vec{G}$, respectively. Hence, $|g|^2 \propto q$ for normal processes and q^{-1} for umklapp $(T > \Theta_1)$. Finally for low temperatures $(T < \Theta_1)$, two plane waves are required to describe the states on the lens surface [Figs. 2(c) and 2(d)]. After a slightly tedious calculation (Sec. III), one finds that $|g|^2 \propto q$ as in the normal process.

In Table I we have collected all the results of the preceding discussion. In the final two rows we tabulated the total q-dependent integrand [except for the factor $f(\omega_q/k_B T)$] and the resulting temperature dependence, respectively. It is interesting to observe that for normal processes and for

umklapp processes at very low temperatures $(T < \Theta_1)$ where distortions of the Fermi surface from sphericity are important, a T^5 law is obtained, although with different coefficients for the two cases. For umklapp processes at sufficiently high temperatures $(T > \Theta_1)$ where we may treat the Fermi surface as spherical, we find a T^2 dependence. If one would take into account, as we do in Sec. II, additional q dependence from the matrix elements, etc., then an additional T^4 term is found. Accordingly, it is impossible to characterize the temperature dependence at low temperature by a single (or simple) power law.

C. Deviations from Matthiessen's Rule

In the preceding discussion (Sec. I B) we have assumed that the deviation function $\Psi(\vec{k})$ was known and given by

$$\Psi_0(\vec{k}) = \vec{v}(\vec{k}) \cdot \hat{E} . \qquad (1.12)$$

If that were the case, then the additivity of the various scattering processes [Matthiessen's rule (MR)] would hold. To see this, note that we can write

$$H = H_{imp} + H_N + H_U , \qquad (1.20)$$

where H_{imp} represents scattering due to impurities (a process not mentioned until now, but very important in most samples), and H_N and H_U represent normal and umklapp electron-phonon scattering, respectively. Accordingly, if (1.12) satisfied (1.8)

$$X = H\Psi_0 ,$$

then (1.11) would be an equality and we would have

$$\rho(\Psi_0) = \rho_{imp}(\Psi_0) + \rho_N(\Psi_0) + \rho_U(\Psi_0) .$$

But in general (1.12) is not a solution of (1.8). Suppose, as is the case in pure Al, that umklapp scattering dominated the resistivity. Now, as we shall see, umklapp scattering is more anisotropic than normal, by which we mean that scattering probability depends strongly on the wave vectors as well as the difference between the wave vectors. Accordingly $\Psi(\vec{k})$ has greater variation than reflected by the simple trial function (1.12)—being more depressed in regions of greater scattering. Let Ψ_U be the solution of the equation

$$X = H_U \Psi_U . \qquad (1.21)$$

Then in the calculation of ρ, the pieces due to umklapp scattering would be considerably less using Ψ_U in place of Ψ_0 [since one can do a variational principle for (1.21)]

$$\rho_U(\Psi_U) < \rho_U(\Psi_0) . \qquad (1.22)$$

Now since $H_U \gg H_{imp}$, H_N (by assumption), the major improvement in calculating ρ_U outweights the

overestimates in ρ_{imp} and ρ_N which occur for using Ψ_U, and we can assert that

$$\rho(\Psi_U) < \rho(\Psi_0) \qquad (1.23)$$

provided that umklapp processes are dominating the resistivity.

Unfortunately we have been using Ψ_0, in our ignorance of Ψ_U. Does that correspond to any physically realizable case? Consider the case of pure impurity scattering. Then the Boltzmann equation has a very simple form

$$\vec{v}(\vec{k}) \cdot \hat{E}e = - \int dS_k \, Q(\vec{k}, \vec{k}')[\Psi(\vec{k}) - \Psi(\vec{k}')] , \quad (1.24)$$

where $Q(\vec{k}, \vec{k}')$ is some effective probability (for elastic scattering) on the Fermi surface. For a *spherical* Fermi surface where we take $Q(\vec{k}, \vec{k}') = Q(|\vec{k} - \vec{k}'|)$ and $\vec{v}(\vec{k}) \sim \vec{k}$, (1.24) can be solved exactly to give

$$\Psi(\vec{k}) = - \tau \, \vec{v}(\vec{k}) \cdot \hat{E}e , \qquad (1.25)$$

where the $\vec{k}$-independent relaxation time τ is

$$1/\tau = \int dS_{k'} \, Q(|\vec{k} - \vec{k}'|)(1 - \hat{k} \cdot \hat{k}') . \qquad (1.26)$$

But clearly (1.25) is just Ψ_0 (up to an irrelevant constant for use in a variational expression for the resistivity). So in the case where impurity scattering dominates, such as in dilute alloys or at the very lowest temperatures, clearly Ψ_0, or (1.25) is nearly the correct deviation function; it is exact for H_{imp}, fairly good for H_N, and rather poor, presumably, for H_U. In any case, we can identify $\rho(\Psi_0)$ with the resistivity for an alloy

$$\rho(\Psi_0) = \rho_{alloy} . \qquad (1.27)$$

On the other hand, we identify

$$\rho(\Psi_U) = \rho_{pure} , \qquad (1.28)$$

since $\Psi = \Psi_U$ is appropriate where umklapp scattering dominates. Accordingly from the inequality (1.23) together with (1.27) and (1.28), we have

$$\rho_{pure} < \rho_{alloy} - \rho_{imp} . \qquad (1.29)$$

The bulk of the difference between the two sides of (1.29) arises from the difference between $\rho_U(\Psi_U)$ and $\rho_U(\Psi_0)$. As we can see from Fig. 1 for Al this amounts to a change of 300% at 20 °K.

In this paper we have not attempted to find the appropriate deviation function for the case of umklapp scattering dominance, Ψ_U. Instead we have always used Ψ_0, so that our calculations should be compared against the experimental results for $\rho - \rho_{imp}$ for *alloys*. When this is done, as may be seen from Fig. 1, the agreement between theory and experiment is considerably improved. We would further suggest that all calculations for polyvalent metals which used Ψ_0 as a trial function should compare their results against experiments for dilute alloys, for which Ψ_0 is more appropriate.

(For alkali metals such as K, deviations from MR are much smaller.) Finally we observe that although we have not done the calculation for Ψ_U, we believe that the mechanism suggested here for deviations from MR is at least as probable as others that have been suggested recently.

We turn now to the plan of the rest of the paper. In Secs. II and III we shall calculate the resistivity from a Fermi surface intersected by only a single set of Bragg planes ($\pm \vec{G}$). In Sec. II, we treat the electronic states as single plane waves, and the Fermi surface as spherical. This is done for simplicity, but it shows that the dominance of umklapp resistivity at low temperatures is essentially a geometrical effect—it requires only that Bragg planes intersect the Fermi surface. The resulting distortion of the Fermi surface is quite incidental. In Sec. III we include approximately the effects of surface distortion and perturbation of electronic states by the Bragg planes. These corrections are important typically for temperatures up to $\sim \Theta_D/10$, and their effect is to reduce the umklapp resistivity. In Sec. IV we attempt to generalize our result to the case in which many Bragg planes intersect the Fermi surface, and to calculate the resistivities of aluminum and indium. Finally, in Sec. V we review general results, and speculate on possible improvements to the theory.

II. SPHERICAL FERMI SURFACE

If the Fermi surface intersects Bragg planes, then umklapp electron-phonon scattering persists at all temperatures and in fact dominates the low-temperature resistivity. The dominance is an essentially geometrical effect—it does not require that the electronic states be perturbed from plane waves. Our effect is therefore well illustrated in this section by treating the electrons as unperturbed by the static lattice. Within this single-plane-wave model umklapp scattering produces pure T^2 and T^4 components in the low-temperature resistivity, which strongly dominate the T^5 from normal scattering.

To begin the discussion we write out in detail the equation for resistivity (1.13). The denominator of (1.13) is given, in general, by

$$(\psi_t, X) = en/m_{opt} \equiv e(12\pi^3 \hbar)^{-1} \int dS_k |\vec{v}(k)| , \quad (2.1)$$

where n is the electron density and m_{opt} is the "optical" effective mass. With the present case of a spherical Fermi surface (FS)

$$m_{opt} = m \quad \text{(spherical FS)}$$

and (1.13) becomes

$$\rho = \frac{m}{ne^2} \left(\frac{3\pi N}{n} \frac{m}{M} S \right) , \qquad (2.2)$$

where

$$S \equiv \frac{\pi}{\hbar} (2\pi q_D^2)^{-3} \iint \frac{dS_k \, dS_{k'}}{|v(k)| \, |v(k')|}$$

$$\times \sum_\lambda (\hbar \omega_{q\lambda})^{-1} f\left(\frac{\hbar \omega_{q\lambda}}{k_B T}\right) \frac{\hbar^2}{m^2} \Pi_\lambda(\vec{k}, \vec{k}') . \quad (2.3)$$

To shorten the writing we have written the product in the integrand of (1.13) as

$$\Pi_\lambda(\vec{k}, \vec{k}') \equiv (m^2/\hbar^2) |\vec{v}(\vec{k}')|^2 |m_\lambda(\vec{k}, \vec{k}')|^2 , \quad (2.4)$$

where m_λ is the matrix element (1.7). We have divided by q_D^6 in (2.3) to give S the unit of inverse time. The relation $q_D^3 = 6\pi^2 N$ together with the factor N^{-1} in (1.13) [see (1.6)] explains the presence of N in the numerator of (2.1).

To prevent the calculation from becoming unwieldy, we make various simplifying assumptions along the way, most of which can be pointed out as they arise. It is appropriate to describe here at the outset, however, our treatment of the phonon frequencies and polarization vectors. We assume a phonon's frequency is proportional to its wave vector $\omega_{q\lambda} \sim |\vec{q}|$, and we allow the "transverse" frequencies ω_{qT} to differ from the "longitudinal" one ω_{qL} but take the two transverse frequencies equal to one another. In the formal expressions (except where noted) we take $\hat{e}_{qL} \sim \vec{q}$ and $\hat{e}_{qT} \cdot \vec{q} = 0$. Since this assumption is not valid except at very small wave vectors, we take the liberty in the actual calculation of averaging over polarization directions $\hat{e}_{q\lambda}$ in the *higher-temperature* corrections. The only important consequence of this average is to multiply the "T^4 term" (which will be derived shortly) by $\frac{5}{3}$. The "T^2 term" ($T > \Theta_1$) would remain unchanged, although the very-low-temperature behavior ($T < \Theta_1$) would be enhanced if we chose to perform the average there. Our treatment of the phonon parameters will be reviewed in Sec. IV with the presentation of results.

To preface our evaluation of S, we digress on the distinction between normal and umklapp scattering. With single-plane-wave electronic states (and a spherical Fermi surface), the normal and umklapp processes are distinguished geometrically, as reflected in S by their separate domains of integration. Our convention will be to work in the extended-reduced zone scheme—that is, for each initial state $\vec{k}$ on the Fermi surface, we sum over all final states $\vec{k}'$ which may lie on the same Fermi surface or on any of the remapped[7] surfaces, but must be separated from $\vec{k}$ by a vector in the first Brillouin zone. As shown on Figs. 2(a) and 2(b), the umklapp processes are those for which $\vec{k}'$ lies on a remapped surface.

For normal processes, we shall be content with reproducing the usual Bloch–Grüneisen formula, which requires (in addition to the approximations

listed above) only that we place the form factor equal to its value at zero argument, $V(0)$. With these approximations, the longitudinal component of Π is

$$\Pi_L = q^4 V^2(0) \quad \text{(normal processes)} \quad (2.5)$$

and the transverse components of Π are zero. The resulting (normal) contribution to resistivity is given by

$$S_N = \frac{V^2(0)}{\hbar k_B \Theta_D} (T/\Theta_D)^5 J_5(\Theta_D/T) , \quad (2.6)$$

where we define the usual Debye temperature,

$$k_B \Theta_D = \hbar c_L q_D , \quad (2.7)$$

with c_L the longitudinal sound velocity. Because it will be useful later, we define the standard functions[8] J_n for general integer n:

$$J_n(x) = \int_0^x \frac{t^n \, dt}{4 \sinh^2 \frac{1}{2} t} . \quad (2.8)$$

For the present case we note that J_5 has the low-temperature limit

$$\lim_{T \to 0} J_5(\Theta_D/T) = J_5(\infty) = 5! \, \zeta(5) = 124.4 .$$

In the case of umklapp processes, the small-q limit of the form factor is $V(G)$,[9] where $\pm \vec{G}$ are the reciprocal-lattice vectors corresponding to the set of Bragg planes of interest. Since $V(G)$ is in many cases quite small, the momentum dependence of V is important in determining the umklapp contribution to resistivity. To partially account for this, we expand V (to first order only) about the small-q limit:

$$V(|\vec{q} + \vec{G}|) = V(G) + \vec{q} \cdot \hat{G} V'(G) , \quad V'(G) = \frac{dV(x)}{dx}\bigg|_{x = G} . \quad (2.9)$$

Using (2.9) to evaluate the matrix elements m_λ [(1.6) and (1.7)] and using the velocity difference function,

$$\vec{v}(\vec{k}') - \vec{v}(\vec{k}) = (\hbar/m)(\vec{q} - \vec{G}) , \quad (2.10)$$

we find that the product Π [defined in (2.4)] is a fourth degree polynomial in q. Denoting as $\Pi^{(n)}$ the term proportional to q^n ($n = 0, 1, \ldots, 4$) we have, for example,

$$\Pi_\lambda^{(0)} = \gamma_\lambda G^4 V^2(G) , \quad \lambda = L, T \quad (2.11a)$$

$$\Pi_T^{(1)} = 2(\vec{q} \cdot \vec{G}) \gamma_T G^2 V(G) [V(G) - G V'(G)] , \quad (2.11b)$$

$$\Pi_T^{(2)} = q^2 G^2 \gamma_T \{ V^2(G) + (\hat{q} \cdot \hat{G})^2 [G^2(V'(G))^2$$

$$- 4 G V'(G) V(G)] \} . \quad (2.11c)$$

The polarization factors γ_λ are defined by

$$\gamma_L = (\hat{q} \cdot \hat{G})^2 \quad \text{and} \quad \sum_T \gamma_T = 1 - \gamma_L \; . \qquad (2.12)$$

Since we are assuming that the two transverse phonon frequencies are equal, it is sufficient to know only the sum of the two transverse polarization factors, rather than each individual factor.

The linear, cubic, and quartic components of Π are strongly dominated by $\Pi^{(2)}$ in their contributions to resistivity (as shown in the Appendix), and we restrict our discussion in the text, therefore, to $\Pi^{(0)}$ and $\Pi^{(2)}$. The contribution to S (2.3) from each component of Π will be denoted separately as $S_\lambda^{(n)}$

$$S_\lambda^{(n)} = \frac{\pi}{\hbar} (2\pi q_D^2)^{-3} \iint \frac{dS \, dS'}{|v| \, |v'|} \; (\hbar \omega_{q\lambda})^{-1} f$$

$$\times \left(\frac{\hbar \omega_{q\lambda}}{k_B T} \right) \frac{\hbar^2}{m^2} \, \Pi_\lambda^{(n)} (\vec{k}, \vec{k}') \; . \qquad (2.13)$$

Then the total S will simply be the sum

$$S = S_N + \sum_{n=0}^{4} \sum_\lambda S_\lambda^{(n)} \; . \qquad (2.14)$$

The evaluation of the surface integrals in the umklapp contributions to S is described in Appendix A, and the results are as follows: First, the contribution from $\Pi_\lambda^{(0)}$ is

$$S^{(0)} = \sum_\lambda S_\lambda^{(0)} = \frac{V^2(G)}{\hbar k_B \Theta_{DL}} \left(\frac{G}{q_D} \right)^3 \left(\frac{T}{\Theta_{DL}} \right)^2$$

$$\times \left[\frac{2}{3} J_2 \left(\frac{\Theta_{DL}}{T} \right) P_2 \left(\frac{\Theta_{2L}}{T}, \frac{\Theta_{DL}}{T} \right) \right.$$

$$\left. + \frac{4}{3} \left(\frac{\Theta_{DL}}{\Theta_{DT}} \right)^3 J_2 \left(\frac{\Theta_{DT}}{T} \right) P_2 \left(\frac{\Theta_{2T}}{T}, \frac{\Theta_{DT}}{T} \right) \right] \; . \qquad (2.15)$$

We introduce a transverse Debye temperature in the same way as the longitudinal one:

$$k_B \Theta_{D\lambda} = \hbar c_\lambda q_D \; . \qquad (2.16)$$

The slowly varying function $P_2(x, y)$ is defined by[10]

$$P_2(x, y) = \frac{1}{2} + \frac{3}{2\pi^2} \int_0^y \frac{z \, dz \, \min(z, x)}{4 \sinh^2 \frac{1}{2} z} \; , \qquad (2.17)$$

and is depicted in Fig 3. P_2 represents a partial cutoff of umklapp scattering phase space at wave vector $2k_F - G$. This wave-vector cutoff defines a characteristic cutoff in temperature,

$$k_B \Theta_{2\lambda} = \hbar c_\lambda (2k_F - G) \qquad (2.18)$$

at which P_2 begins to drop from its low-temperature limit of unity. Since the low-temperature limit of J_2 is $\pi^2/3$, the low-temperature limit of $S^{(0)}$ is

$$\lim_{T \to 0} S^{(0)} = \frac{2\pi^2}{3} \frac{V^2(G)}{\hbar k_B \Theta_{DL}} \left(\frac{G}{q_D} \right)^3 \left(\frac{T}{\Theta_{DL}} \right)^2 \left[\frac{1}{3} + \frac{2}{3} \left(\frac{\Theta_{DL}}{\Theta_{DT}} \right)^3 \right] \; . \qquad (2.19)$$

Since Θ_{DL} is roughly twice Θ_{DT} (typical values are given on Table II), the transverse contribution to $S^{(0)}$ dominates the longitudinal contribution by roughly a factor of 16. Since $S_T^{(2)}$ dominates $S_L^{(2)}$ by an even larger factor, we shall restrict our discussion to the transverse components in our treatment of umklapp processes. Again referring to Appendix A for the surface integrations, we find that

$$S_T^{(2)} = \frac{4}{15} \frac{G}{q_D} \left(\frac{T}{\Theta_{DT}} \right)^4 J_4 \left(\frac{\Theta_{DT}}{T} \right) P_4 \left(\frac{\Theta_{2T}}{T}, \frac{\Theta_{DT}}{T} \right)$$

$$\times \frac{[GV'(G)]^2}{\hbar k_B \Theta_{DT}} \left[1 - \frac{4V(G)}{GV'(G)} + \frac{5}{2} \frac{P_4'}{P_4} \left(\frac{V(G)}{GV'(G)} \right)^2 \right] \; . \qquad (2.20)$$

The partial cutoff of umklapp scattering phase space is represented by P_4 and P_4' [11]:

$$P_4(x, y) = \frac{1}{2} + \frac{90}{48\pi^4} \int_0^y z \, dz \, \min(z, x)$$

$$\times [az^2 + (1-a)\min^2(z, x)] \; , \qquad (2.21)$$

$$a = \tfrac{3}{2} (1 - G^2/4k_F^2) \; .$$

P_4' is very similar to P_4, and multiplies an unimportant factor in (2.20). The low-temperature limit of both is unity. Since the low-temperature limit of J_4 is $24\pi^4/90$, we have

$$\lim_{T \to 0} S_T^{(2)} = \frac{4}{15} \frac{24\pi^4}{90} \frac{G}{q_D} \left(\frac{T}{\Theta_{DT}} \right)^4 \frac{[GV'(G)]^2}{\hbar k_B \Theta_{DT}}$$

$$\times \left[1 - \frac{4V(G)}{GV'(G)} + \frac{5}{2} \left(\frac{V(G)}{GV'(G)} \right)^2 \right] \; . \qquad (2.22)$$

Three points should be made: (i) The low-temperature limit of the resistivity is a polynomial in T, the dominant umklapp contributions being proportional to T^2 and T^4, and the normal contribution proportional to T^5; (ii) the normal contribution is strongly dominated by the umklapp contribution over the entire temperature range for which our treatment is valid; (iii) finally, deviations from the
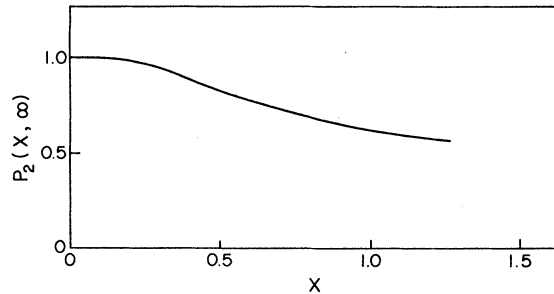

FIG. 3. Partial cutoff of umklapp scattering phase space.

TABLE II. Listed values of the characteristic temperatures Θ_1 and Θ_2 correspond to the Bragg planes (200) of aluminum and (111) of indium, which provide the dominant umklapp contributions to the resistivity of each metal.

	Θ_D (°K)[a]	Dominant Bragg planes (G)	$\frac{G}{k_F}$	$\frac{|V(G)|^{[b]}}{E_F}$	$\frac{GV'(G)}{E_F}$	Θ_1 (°K)	Θ_2 (°K)
Al	395	(200)	1.77	0.066	0.33	26	104
In	90	(111)	1.54	0.076	0.47	7	47

$$\frac{\Theta_1}{\Theta_D} = \frac{|V(G)|}{E_F} , \quad \frac{\Theta_2}{\Theta_D} = \frac{2k_F - G}{q_D}$$

[a]In our work we shall take Θ_{DT} to be equal to the "experimental" values of Θ_D tabulated above, which are found in Ref. 5 for Al, and in Ref. 1 for In. The tabulated values are close to those determined from transverse sound velocities. The values calculated from longitudinal sound velocities are roughly twice as great.

[b]See Ref. 9.

T^2 and T^4 power laws, represented by P_2 and P_4, are to be expected at temperatures near Θ_{2T}, which is considerably less than Θ_{DL} or Θ_{DT}. For typical examples see Table II.

The polynomial form of resistivity in the low-temperature limit is a consequence of the single-plane-wave approximation. As mentioned in the Introduction, the effect of admixing a second plane wave in the vicinity of the Bragg planes is to suppress the umklapp contribution to resistivity for temperatures below the characteristic temperature Θ_{1T}. Only for somewhat higher temperatures does the polynomial form (with partial cutoffs at Θ_{2T}) remain valid.

To conclude this section we warn that the T^2 term $S_T^{(0)}$ may not be recognizable experimentally. Identification of $S_T^{(0)}$ would require that the polynomial form of S be quite fully developed at temperatures low enough that $S_T^{(0)}$ be comparable with or greater than $S_T^{(2)}$. In our study of specific cases we shall find that this requirement is not fulfilled.

III. DISTORTED FERMI SURFACE

In this section we describe an approximate method for including the essential effect of the perturbation on electronic states induced by a pair of Bragg planes which intersect the Fermi surface. To give a brief preview, the result of using two-plane-wave electronic states is that for energy-conserving transitions, both the velocity difference $\vec{v}' - \vec{v}$ and the squared matrix element $m_\lambda^2(\vec{k}', \vec{k})$ go to zero linearly as reduced wave vector q goes to zero. This in turn means that the limiting low-temperature resistivity is proportional to T^5. The T^2-like behavior begins at such temperatures that typical phonon wave vectors exceed the scale of Fermi-surface distortion, $q \sim k_F V(G)/E_F$. So the characteristic temperature is roughly $\Theta_{1T} \sim \Theta_{DT} V(G)/E_F$.

Typical values of Θ_{1T} are given in Table II.

Before going on, we mention an effect not included in our treatment—the increased m_{opt}, (2.1), resulting from Fermi-surface distortion. The reason it is not included is that there are comparable corrections to S, (2.2), which cannot easily be included in our treatment, but which tend to cancel the m_{opt} increase. Moreover, we estimate that the final result, with all its approximations, is valid only to within about a factor of 2. We feel that the smaller numerical corrections[12] such as m_{opt} are therefore unwarranted. One might nevertheless argue that since we are calculating an "upper bound" to resistivity (1.11) we ought to use an upper bound to the value of m_{opt}. However, this calculation is intended as an upper bound in the sense of (1.29), i.e., as the temperature-dependent resistivity of an alloy as opposed to that of a pure metal.

Before discussing the computation of S, we review the two-plane-wave formalism for an electronic state in the vicinity of the Bragg plane (G). We write the wave function

$$\psi_k(r) = e^{i\vec{k} \cdot \vec{r}} \sin\theta + e^{i(\vec{k}-\vec{G}) \cdot \vec{r}} \cos\theta . \qquad (3.1)$$

In a basis where ψ_k is written $\binom{\sin\theta}{\cos\theta}$, the (truncated) pseudo-Hamiltonian matrix is

$$[H] = \begin{bmatrix} \dfrac{\hbar^2 k^2}{2m} & V(G) \\ V(G) & \dfrac{\hbar^2 (k-G)^2}{2m} \end{bmatrix} . \qquad (3.2)$$

We diagonalize H by the choice

$$\tan\theta_\pm = \eta \pm \text{sgn}[V(G)] (\eta^2 + 1)^{1/2} , \qquad (3.3a)$$

where

$$\eta = \frac{\hbar^2}{2m V(G)} (\vec{k} \cdot \vec{G} - \tfrac{1}{2} G^2) . \qquad (3.3b)$$

η is a measure of the "distance" of $\vec{k}$ from the Bragg plane (G), and will be frequently referred to in this sense. We write the wave functions corresponding to Eq. (3.3a) as $\psi_k^{(\pm)}(r)$, with (+) to denote the upper band and (−) to denote the lower band. The energies and velocities are

$$E(\vec{k})^{(\pm)} = \langle \psi_k^{(\pm)} | H | \psi_k^{(\pm)} \rangle = \hbar^2 k^2 / 2m + V(G) \cot\theta_\pm ,$$
$$\qquad (3.4)$$

$$\vec{v}(\vec{k})^{(\pm)} = \left\langle \psi_k^{(\pm)} \left| \frac{\hbar \nabla}{mi} \right| \psi_k^{(\pm)} \right\rangle = \vec{k} - \vec{G} \cos^2\theta_\pm = \frac{1}{\hbar} \frac{\partial E(k)^{(\pm)}}{\partial \vec{k}} . \qquad (3.5)$$

The second-zone Fermi surface is given by $E_k^{(+)} = E_F$, and the first-zone surface by $E_k^{(-)} = E_F$, as shown in Fig. 4. The matrix elements $m_\lambda(\vec{k}'\pm, \vec{k}\pm) = \langle \psi_{k'}^{(\pm)} | \hat{\epsilon}_{q\lambda} \cdot \nabla V | \psi_k^{(\pm)} \rangle$ are given by

$$- im_L(\vec{k}', \vec{k}) = qV(q)(SS' + CC')$$

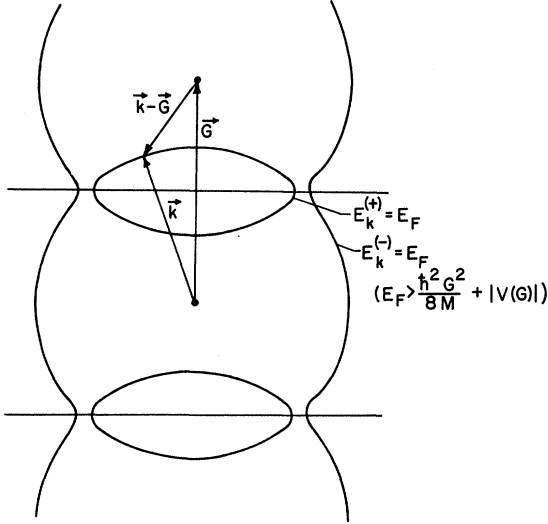FIG. 4. Distorted Fermi surface, with (±) band indexes indicated.

$$+ qV(q - G)SC' + qV(q + G)S'C$$

$$+ \hat{q} \cdot \vec{G}[V(q + G)S'C - V(q - G)SC'] , \quad (3.6a)$$

$$\sum_T |m_T(\vec{k}', \vec{k})|^2 = G^2(1 - \gamma_L)[V(q + G)S'C$$

$$- V(q - G)SC']^2 , \quad (3.6b)$$

where

$$S' = \sin\theta(\vec{k}'), \quad C' = \cos\theta(\vec{k}'), \text{ etc.} \quad (3.6c)$$

The band indices (±) are carried by the coefficients S and C; (3.6a) and (3.6b) are otherwise independent of the band indices (see Fig. 5).

Treating momentum dependence of the form factor as in Sec. II, and using (3.5) and (3.6), we write the product Π as defined by (2.4). Because of implicit q dependence in the mixing coefficients S and C, Π is no longer strictly a polynomial in q. So we define as $\Pi^{(n)}$ the term *explicitly* proportional to q^n, and obtain, for example,

$$\Pi_\lambda^{(0)} = \gamma_\lambda G^4 V^2(G) \sin^2(\theta' - \theta)(C'^2 - C^2)^2 , \quad (3.7a)$$

$$\Pi_T^{(1)} = 2(\vec{q} \cdot \vec{G})G^2 \gamma_T (C'^2 - C^2)[V^2(G) \sin^2(\theta' - \theta)$$

$$- (C'^2 - C^2)^2 GV'(G)V(G)] , \quad (3.7b)$$

and

$$\Pi_T^{(2)} = q^2 G^2 \gamma_T \{(\hat{q} \cdot \hat{G})^2 [(C'^2 - C^2)^2 G^2(V'(G))^2 \sin^2(\theta' - \theta)$$

$$- 4(C'^2 - C^2)^2 GV'(G)V(G)] + V^2(G) \sin^2(\theta' - \theta)\} . \quad (3.7c)$$

In this section we shall distinguish a given contribution to resistivity (or equivalently, a given term in Π) as normal or umklapp, even though a given scattering process cannot be so distinguished unless both $\vec{k}$ and $\vec{k}'$ are far removed from both of

the Bragg planes. Our classification is as follows: We define as normal, one of the several terms in $\Pi_L^{(4)}$:

$$\Pi_N \equiv q^4 V^2(q)(SS' + CC') , \quad (3.8)$$

and we define everything else as umklapp:

$$\Pi_U \equiv (\Pi_L^{(4)} - \Pi_N, \Pi_\lambda^{(n)}), \quad n = 0, \ldots, 3 .$$

The reason for this ostensibly arbitrary assignment is clear from the asymptotic forms of Π for $\vec{k}$ and $\vec{k}'$ far removed from the Bragg planes. [$|\eta|$ and $|\eta'|$, (3.3b), large.] Referring to Fig. 5 for the asymptotic values of the angle θ, one can verify that for $\vec{k}$ and $\vec{k}'$ both on the *un*remapped Fermi surface (a normal process in the sense of Sec. II):
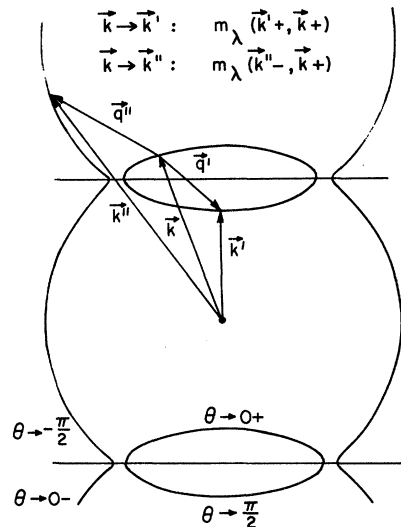
$$\Pi_N \to q^4 V^2(q)[1 + O(\eta^{-2})] , \quad \Pi_U \to O(\eta^{-2}) .$$

For $\vec{k}'$ on a remapped surface (an umklapp process in the sense of Sec. II), we have

$$\Pi_N \to O(\eta^{-2}) ,$$

$$\Pi_{U\lambda}^{(n)} \to (\Pi_{spw})_\lambda^{(n)} [1 + O(\eta^{-2})] .$$

That is, each component of Π_U approaches asymptotically the value of the corresponding single-plane-wave (spw) component of Π. In particular, the limiting large-$|\eta|$ forms of $\Pi_\lambda^{(0)}$, $\Pi_T^{(1)}$, and $\Pi_T^{(2)}$ [(3.7a)–(3.7c)] are given by (2.11a)–(2.11c).

$$\vec{q}', \vec{q}'' \text{ both in 1st B.Z.}$$

Asymptotic values of θ
as $|\eta| \to \infty$, for $V(G) > 0$.

FIG. 5. Examples of umklapp scattering on a distorted Fermi surface. Asymptotic values (for large η) of the parameter θ are shown. θ is understood as θ_+ on the second-zone surface, and as θ_- on the first-zone surface.

We shall also require the small-q asymptotic form of (3.7a). For sufficiently small q, only intraband processes can conserve energy [Figs. 2(c) and 2(d)]. It follows from (3.3), therefore, that $\Delta\theta \equiv \theta' - \theta \to 0$ as $q \to 0$, and that to lowest order in $\Delta\theta$ (3.7a) becomes

$$\Pi_\lambda^{(0)} \to \gamma_\lambda G^4 V^2(G) (2\sin\theta \cos\theta)^2 (\Delta\theta)^4 . \qquad (3.9)$$

We write $\Delta\theta$ in terms of $\vec{q}$ by using two identities: from (3.3a)

$$\frac{d\theta}{d\eta} = 2\sin^2\theta \cos^2\theta = \tfrac{1}{2}(\eta^2 + 1)^{-1} , \qquad (3.10a)$$

and from (3.3b)

$$\Delta\eta \equiv \eta' - \eta = \frac{\hbar^2}{2mV(G)} (\vec{q} \cdot \vec{G}) \qquad (3.10b)$$

for both $(\pm)$ bands. So

$$\lim_{q \to 0} \Delta\theta = \frac{E(G)}{V(G)} \frac{\vec{q} \cdot \vec{G}}{G^2} \frac{1}{2(\eta^2 + 1)} , \qquad (3.11)$$

where $E(G) \equiv \hbar^2 G^2/2m$, and (3.9) is

$$\lim_{q \to 0} \Pi_\lambda^{(0)} = \gamma_\lambda \frac{(\vec{q} \cdot \vec{G})^4}{G^4} \frac{E^4(G)}{V^2(G)} \frac{2}{[2(\eta^2 + 1)]^5} . \qquad (3.12)$$

As with normal processes [(2.5) and (3.8)] the quartic q dependence leads to a T^5 temperature dependence in $S^{(0)}$. However, the coefficient of T^5 is larger in $S^{(0)}$ than in S_N, even if the transverse Debye temperature is used in both. Ignoring the η dependence in (3.12) gives

$$\lim_{q \to 0} \Pi_\lambda^{(0)}/\Pi_N \sim E^2(G)/V^2(G) .$$

The effect of the η dependence is to restrict the contribution of the surface integral $\int dS$ in the expression for $S_\lambda^{(0)}$, (2.13), to the regions near the Bragg planes. The fraction of the surface which contributes is of order $V(G)/E(G)$, so in fact

$$\lim_{T \to 0} S_\lambda^{(0)}/S_N \sim E(G)/V(G) . \qquad (3.13)$$

The inverse proportionality to $V(G)$ indicates that the Bragg planes with the smallest band gap may dominate the very low-temperature behavior. As a result the temperature regime in which the T^5 behavior is realized is determined by the smallest band gap of the metal ($T \ll$ smallest Θ_1).

It is instructive to compare the low-temperature asymptote of $S_\lambda^{(0)}$, (3.13), with its $T > \Theta_1$, or spw form (2.15):

$$\lim_{T \to 0} S_\lambda^{(0)}/(S_{\text{spw}})_\lambda^{(0)} \sim \left(\frac{E(G)}{V(G)} \frac{T}{\Theta_{D\lambda}} \right)^3 . \qquad (3.14)$$

The temperature at which the two asymptotic forms of $S_\lambda^{(0)}$ are equal is

$$T \sim [V(G)/E(G)] \Theta_D \sim \Theta_1$$

$[E(G)$ is of the same order of magnitude as $E_F]$. So

as we have said, it is Θ_1 which separates the two power-law regimes of $S_\lambda^{(0)}$.

From the foregoing a general property of $S_\lambda^{(0)}$ is apparent. If we make the Debye approximation and ignore the cutoffs Θ_2 and Θ_D, then for a given species of Bragg planes $S_\lambda^{(0)}$ is the product of the single-plane-wave form and a function F of $k_B T/V(G)$ only:

$$S_\lambda^{(0)} = (S_{\text{spw}})_\lambda^0 F_\lambda(k_B T/V(G)) . \qquad (3.15)$$

Since $(S_{\text{spw}})_\lambda^0 \sim V^2(G)T^2$ it follows from (3.15) that if the low-temperature asymptote is proportional to T^5, it must also be proportional to $V^{-1}(G)$. It also follows that the "change-over" temperature Θ_1 is proportional to $V(G)$.

In order to calculate $S_T^{(0)}$ over the entire temperature region $T \ll \Theta_D$, we have used the following scheme for approximating the surface integrals of (2.13). We introduce a temperature-independent interpolation function $I(q)$ defined by

$$S_T^{(0)} \equiv (\hbar q_D)^{-1} \int_0^\infty dq \, (\hbar\omega_{qT})^{-1} f\left(\frac{\hbar\omega_{qT}}{k_B T}\right) I(q) . \qquad (3.16)$$

Precisely defined, $I(q)$ is the double surface integral (2.13) over $\vec{k}$ and $\vec{k}'$ subject to $|\vec{k}' - \vec{k}| = q$. Our scheme is to interpolate between the small-q asymptotic form of $I(q)$, which we calculate analytically from (3.12),

$$\lim_{q \to 0} I(q) \sim q^5/V(G) , \qquad (3.17)$$

and the large-q form which we take to be the single-plane-wave function (A11)

$$I_{\text{spw}}(q) = \tfrac{2}{3} V^2(G)(G/q_D)^3 q[q + \min(q, q_2)]/q_D^2 . \qquad (3.18)$$

The interpolation is shown on Fig. 6, using (3.18) as a scale of reference. The step function represents the onset of interband transitions at the interband threshold wave vector

$$q_{\text{int}} = k_F \frac{V(G)}{E_F} \left[1 - \left(\frac{G}{2k_F} \right)^2 \right]^{-1/2} . \qquad (3.19)$$

For $q < q_{\text{int}}$ we allow the small-q form to saturate at only half the large-q form, assuming the phase space to be roughly equally divided between intraband and interband scattering near the threshold.

The interpolation function $I(q)$ manifests the property (3.15). It is clear from (3.19) that for different geometries (G/k_F), different functions F are required in (3.15).

On Fig. 7 we have plotted the contributions to resistivity $S_T^{(0)}$ resulting from our approximations to I. Again the plots are appropriate to the geometry and band gap of the (111) and (200) planes of aluminum. In Sec. IV we shall apply the results to Al and In.
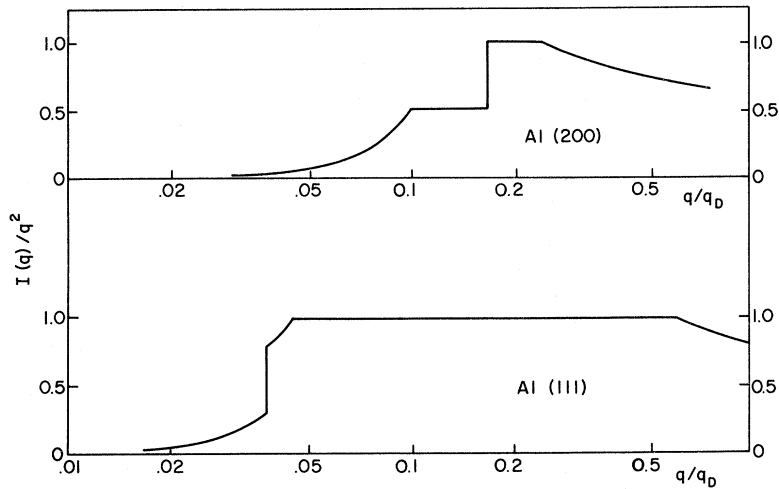
FIG. 6.   Interpolation between high-
and low-q asymptotes of $I(q)$.

IV. APPLICATION TO ALUMINUM AND INDIUM

If a Fermi surface intersects many Bragg
planes, the same method for counting states dis-
cussed in previous sections still applies: For each
initial state $\vec{k}$ on the Fermi surface, we sum over
final states $\vec{k}'$ which may lie on the Fermi surface,
or on any of the remapped surfaces; but $\vec{k}' - \vec{k}$ is
restricted to the first Brillouin zone. We there-
fore estimate the total umklapp contribution to re-
sistivity by adding together the separate contribu-
tions from each pair of Bragg planes. Our ignor-
ance of the effect of states which require three or
four plane waves for their description is the only
new approximation introduced by this procedure.
Except near points of contact between second- and
third-zone Fermi surfaces, the continuity of veloc-
ity and vanishing small-q transition probability
remain intact, so the resistivity is not altered sig-
nificantly.

One special feature we *do* account for is the ab-
sence of much of the third-zone Fermi surface of
indium, as described in Table III. The third-zone

arms which lie along the edges of the rhombohedral
(200) faces of the zone are almost completely re-
moved by the lattice potential. This precludes in-
terband transitions near the (200) faces, and re-
moves half of the intraband contribution to ρ_U at
low temperatures. Since the edges of (200) zone
faces comprise two-thirds of the edges of the (111)
faces, the contribution to ρ_U from (111) planes is

TABLE III.   The number of pairs of each species of
the Bragg plane is listed, together with the fractional re-
duction in the intraband and interband contributions from
each pair. There is no reduction in aluminum, and in
indium the reduction results from the near absence of
segments of the third-zone Fermi surface which border
the (200) faces of the Brillouin zone.

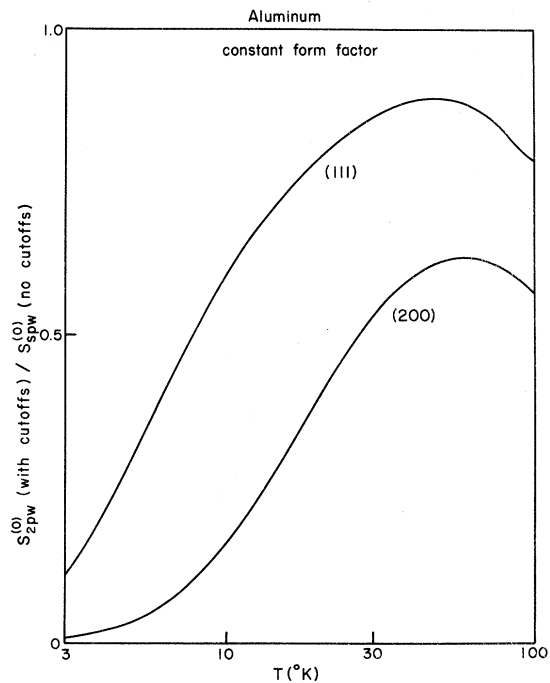|	Plane	(200)	(002)	(111)
In	No. of pairs	2	1	4
	Weight	Intraband $\frac{1}{2}$	1	Intraband $\frac{2}{3}$
		Interband 0		Interband $\frac{1}{3}$
Al	No. of pairs	3		4

FIG. 7. $S_T^{(0)}$ resulting from a pair of (111) planes, and
from a pair of (200) planes in aluminum. We have plotted
the ratio of $S_T^{(0)}$ with both high-temperature and low-tem-
perature cutoffs, to the same quantity with neither of the
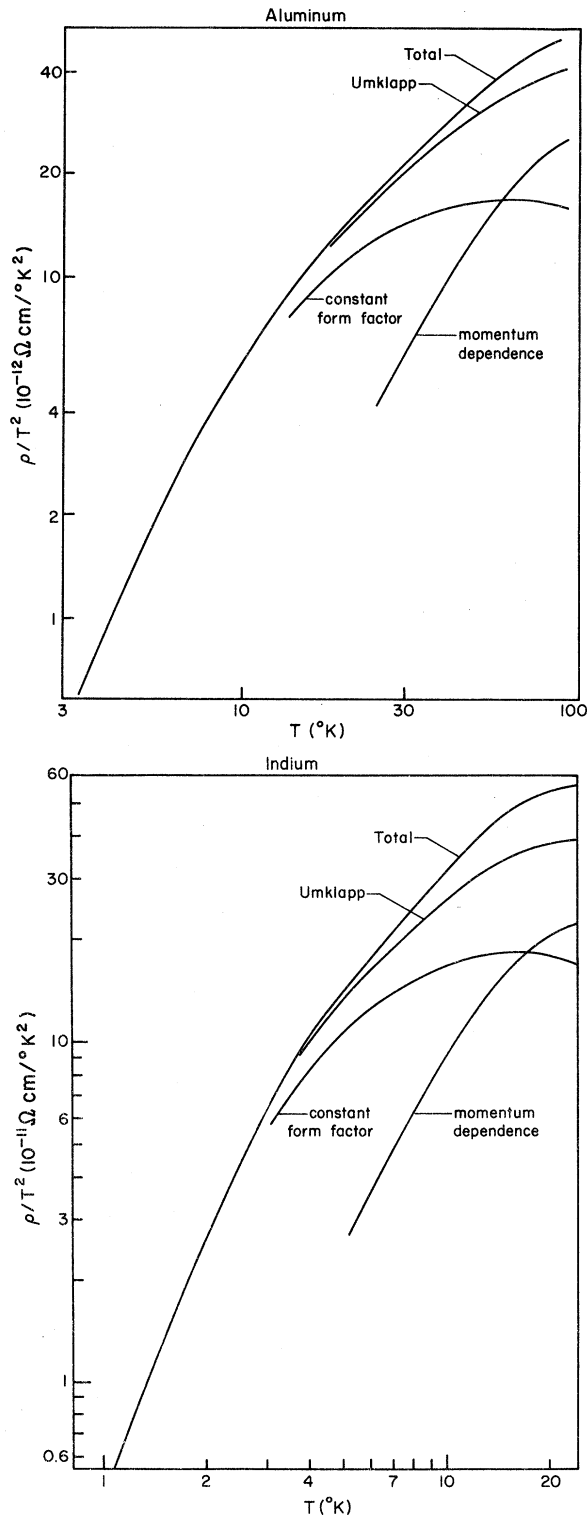cutoffs.

Aluminum

40

20

ρ/T^2 ($10^{-12}\,\Omega\,\text{cm}/{}^{\circ}\text{K}^2$)

10

Total

Umklapp

constant form factor

momentum dependence

4

2

1

3   10   30   100

T (°K)

Indium

60

30

Total

Umklapp

ρ/T^2 ($10^{-11}\,\Omega\,\text{cm}/{}^{\circ}\text{K}^2$)

10

6

constant form factor

momentum dependence

3

1

0.6

1   2   4   7   10   20

T (°K)

FIG. 8. ρ/T^2 for aluminum and indium. The separate umklapp contributions are shown: the "T^2 term" result-ing from a constant form factor, and the "T^4 term" resulting primarily from the momentum dependence of the form factor [more precisely, momentum dependence of Π, Eq. (2.4)].

also reduced, as shown in the table.

The results of our calculation are shown on Fig. 8, where we have plotted resistivity divided by T^2 to accentuate the low-temperature behavior. The umklapp contribution is broken into its "T^2" and "T^4" components, to show in what temperature regime each is important. As in Fig. 1 the total resistivity is obtained by adding a "normal" contribution to the umklapp contribution developed here. The "normal" contribution is given by the Bloch–Grüneisen formula, and the transverse Debye temperature Θ_{DT} is used. Since the "T^4" components are important only at higher temperatures, we performed an average over phonon polarizations in evaluating them. The effect is to multiply $S_T^{(2)}$ [(2.20) and (2.22)] by the factor $\frac{5}{3}$. The strength of the "T^2" term is independent of the polarization directions, but the low-temperature cutoffs below Θ_{1T} are quite sensitive. In evaluating the low-temperature asymptote we therefore assumed that the low-frequency modes were purely transverse. This assumption minimizes the coefficient of the T^5 asymptote.

Focusing on aluminum, the following features deserve special comment: (i) The T^4 term, representing largely the momentum dependence of the form factor $V(q)$, is unimportant below about 20 °K. However, it does become important before the T^2 term is fully developed, precluding experimental isolation of a T^2 component in the total resistivity. (ii) The low-temperature resistivity is not well represented over any sizable temperature range by a power law or a polynomial in temperature. The ultimate low-temperature form T^5 is achieved only for temperatures below about 3 °K in aluminum. In the 4–10 °K range the behavior is roughly T^4, and an approximate T^3 dependence occurs in the 20–40 °K range.

From Fig. 1 we see that the inclusion of umklapp scattering improves both the qualitative and quantitative agreement with experiment over the agreement obtained using the Bloch–Grüneisen formula alone, even when the transverse Debye temperature is used in the Bloch–Grüneisen formula. Recall from Sec. I that this theory and all such calculations for polyvalent metals must be compared with the measured resistivities of dirty metals. Having completed our calculation, it is appropriate to repeat its interpretation here.

A. Interpretation

The predominance of umklapp scattering between states close to the Bragg planes tends to produce a highly anisotropic relaxation time. The effect of impurities is to reduce the degree of anisotropy in the total scattering time. According to the variational principle, this will increase the (temperature-dependent) resistivity due to electron-phonon

scattering. Our present calculation, through its choice of a trial distribution function (1.12) used in the resistivity formula (1.11), assumes an isotropic relaxation time τ, and therefore represents the "dirty limit" temperature-dependent resistivity. In a clean metal, the umklapp-induced anisotropy must be reflected in the trial distribution function. According to the variational principle, the improved trial function will reduce the temperature-dependent resistivity.

This interpretation suggests that the measured resistivities of dirty samples can be understood as resulting primarily from electron-phonon scattering, and that it is unnecessary to invoke other mechanisms, such as perturbation of the electron-phonon transition amplitudes by impurities.[3,13] The impurities are necessary only to support an approximately isotropic relaxation time. The reduction of temperature-dependent resistivity in cleaner samples can be understood qualitatively as a breakdown of the relaxation-time approximation due to anisotropy. This conclusion is supported by the observation that the effect is more pronounced in polyvalent metals than in potassium,[14] for example, where the umklapp-induced anisotropy is less. While other mechanisms may be present, none leading to the large observed effects have yet been proposed. For example, a breakdown of the momentum-conservation condition for electron-phonon scattering due to the presence of impurities has been shown to lead to a negligible contribution to the observed deviations from MR.[3,13]

Before terminating this section we cite the work of Pytte,[15] who uses two-plane-wave electronic states and experimental phonon dispersion curves in his calculation of resistivity for aluminum. Since he omits from his surface integrations the regions close to the Bragg planes, his calculation is not accurate below about 20–30 °K. It is interesting to note that his calculated resistivity is proportional to roughly T^4 in the 30 °K regime, and that it falls between the "dirtiest" and "cleanest" experimental resistivities plotted on Fig. 1(a).

V. CONCLUSIONS

Despite its many approximations, the present study of umklapp electron-phonon scattering suggests a possible explanation for observed resistivities of dirty polyvalent metals. The following conclusions briefly summarize the study. Treating the momentum dependence of the scattering form factor to first order has resulted in T^2 and T^4 terms in the resistivity. These umklapp contributions are not extinguished exponentially at low temperatures as in the alkalis, but they are suppressed (due to Fermi-surface distortion) and their ultimate low-temperature behavior is T^5. Because of the suppression, the T^2 term may not be dis-

cernible, as we have found to be the case in Al and In, where in the $T \lesssim \frac{1}{10}\Theta_D$ regime the total resistivity appears to be proportional to T^3, or perhaps even T^4. Finally, the low-temperature limit, proportional to T^5, far exceeds the normal contribution to resistivity, so the umklapp contribution dominates at all temperatures.

Our theory does not quantitatively account for impurity dependence of the temperature-dependent resistivity, but it dramatizes the highly anisotropic nature of umklapp scattering, and leads us to suggest that the deviations from MR are manifestations of the breakdown of the relaxation-time approximation. The present calculation, with its simple trial distribution function, is appropriate to the electron-phonon-limited resistivity of a dirty metal.

APPENDIX

We are concerned here with the evaluation of the quantity S which, from its definition (2.3) and noting that

$$(\hbar\omega)^{-1} f(\beta\hbar\omega) = (4k_B T \sinh^2 \tfrac{1}{2}\beta\hbar\omega)^{-1} , \qquad \beta = 1/k_B T$$

can be written

$$S = \frac{\pi}{\hbar k_B T} (2\pi q_D^2)^{-3} \iint \frac{dS \, dS'}{|v| \, |v'|} \sum_\lambda \frac{(\hbar^2/m^2) \Pi_\lambda(\vec{k}', \vec{k})}{4 \sinh^2 \tfrac{1}{2}\beta\hbar\omega_{q\lambda}} ,$$

(A1)

where

$$\Pi_\lambda(\vec{k}', \vec{k}) = (m^2/\hbar^2)|\vec{v}' - \vec{v}|^2 |m_\lambda(\vec{k}', \vec{k})|^2 . \qquad (A2)$$

We limit ourselves to the case under study in Sec. II of the text—a spherical Fermi surface with single-plane-wave electronic states, intersected by a single pair of Bragg planes ($\pm\vec{G}$). Although we are particularly interested in umklapp processes, we first evaluate the more familiar contribution from normal processes.

For normal processes, the product Π is given by

$$\Pi_L = q^4 V^2(q) \quad \text{and} \quad \Pi_T = 0 \quad (q = |\vec{k}' - \vec{k}|) . \qquad (A3)$$

Since the integrand in (A1) depends only on the magnitude of momentum transfer $|\vec{k}' - \vec{k}|$, we write one of the surface integrals, say S', as
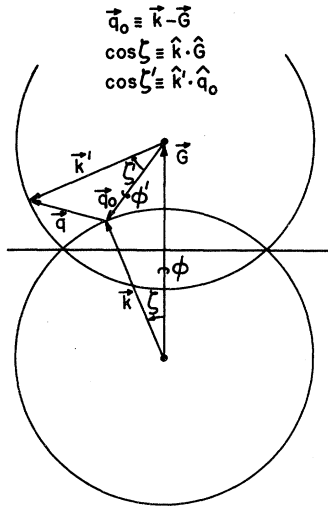
$$\int dS' \rightarrow 2\pi \int_0^{q_D} q \, dq .$$

The limits of q integration are independent of $\vec{k}$, so the S integration trivially contributes the Fermi-surface area, and the double surface integral can be written

$$\iint dS \, dS' \rightarrow 8\pi^2 k_F^2 \int_0^{q_D} q \, dq , \qquad (A4)$$

to display the phase space for normal scattering as written in Table I of the text. The normal contribution to S is therefore
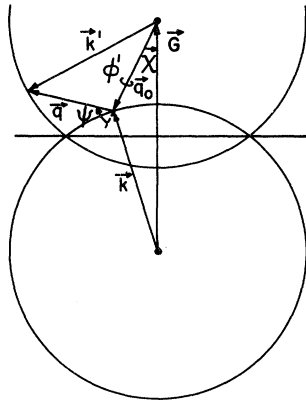
$$S_N = \frac{1}{\hbar k_B T} \int_0^{q_D} \frac{q^5 dq}{q_D^6} V^2(q) \frac{1}{4 \sinh^2 \beta \hbar \omega_L} \quad .$$

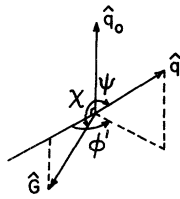Putting $V(q)$ equal to $V(0)$ results in the Bloch–

$$\vec{q}_0 \equiv \vec{k} - \vec{G}$$
$$\cos\zeta \equiv \hat{k} \cdot \hat{G}$$
$$\cos\zeta' \equiv \hat{k}' \cdot \hat{q}_0$$

(a)

$$\cos\psi \equiv \hat{q} \cdot \hat{q}_0$$
$$\cos\chi \equiv \hat{G} \cdot \hat{q}_0$$

$$\hat{q} \cdot \hat{G} = \cos\chi \cos\psi + \cos\phi' \sin\chi \sin\psi$$

(b)

FIG. 9. Angular variables for surface integrations.

Grüneisen formula (2.6).

Turning to umklapp processes, we discuss first the manipulation of the surface integrals. For a given $\vec{k}$ on the Fermi surface, we permit $\vec{k}'$ to range over the remapped surface, as shown on Fig. 2, but constrain the reduced momentum transfer q to be less than q_D. Referring to Fig. 9(a) we rewrite the double surface integral:

$$dS \, dS' = k_F^4 \sin\zeta \, d\zeta \, d\phi \sin\zeta' \, d\zeta' \, d\phi' \quad , \tag{A5}$$

where the angles, as shown in the figure, are defined by

$$\cos\zeta \equiv \hat{k} \cdot \hat{G},$$

$$\cos\zeta' \equiv \hat{k}' \cdot \hat{q}_0, \quad \vec{q}_0 \equiv \vec{k} - \vec{G} \quad .$$

We convert the ζ and ζ' integrations to integrals over the magnitudes of $\vec{q}$ and $\vec{q}_0$, which we denote by q and q_0, respectively. For fixed $\vec{k}$ (fixed ζ and ϕ) the expression

$$q^2 = k'^2 + q_0^2 - 2k' q_0 \cos\zeta' \quad ,$$

leads to

$$(q/q_0) \, dq = k_F \sin\zeta' \, d\zeta' \quad . \tag{A6}$$

Next, the expression for q_0,

$$q_0^2 = k^2 + G^2 - 2kG \cos\zeta \quad , \tag{A7}$$

leads to

$$q_0 dq_0 = k_F G \sin\zeta \, d\zeta \quad .$$

Finally, from cylindrical symmetry the ϕ integration trivially contributes 2π, so from (A5)–(A7)[16]:

$$dS \, dS' = 2\pi (k_F^2/G) \, dq_0 q \, dq \, d\phi' \quad . \tag{A8}$$

q varies from $k_F - q_0$ (the shortest distance from $\vec{k}$ to the "remapped surface") to q_D, and q_0 varies from $G - k_F$ to $k_F + q_D$. Since q and q_0 vary between these limits at *each* Bragg plane, we multiply by two and

$$\int \int dS \, dS' = (4\pi k_F^2/G) \int_{G-k_F}^{k_F+q_D} dq_0 \int_{|k_F-q_0|}^{q_D} q \, dq \int_0^{2\pi} d\phi' \quad . \tag{A9}$$

To simplify the expression we change variables, $q_0 = p + k_F$, to get

$$\int \int dS \, dS' = (4\pi k_F^2/G) \int_{G-2k_F}^{q_D} dp \int_{|p|}^{q_D} q \, dq \int_0^{2\pi} d\phi' \quad . \tag{A10}$$

We can derive the form of the umklapp scattering phase space (Table I) by assuming the integrand is independent of p and ϕ': The angular integration gives 2π, and the p integration is done by parts to yield

$$\int \int dS \, dS' = (8\pi^2 k_F^2/G) \int_0^{q_D} q^2 \, dq[1 + \min(1, q_2/q)] \quad ,$$

$$q_2 \equiv 2k_F - G. \tag{A11}$$

The cutoff at $2k_F - G$ represents the partial cutoff of umklapp scattering phase space discussed in the text.

The integrand in (A1) does, of course, depend on p and ϕ', through the factor $\Pi(\vec{k}', \vec{k})$. To make the dependence explicit, we note that Π can be written as a sum of terms proportional to $q^n(\vec{q} \cdot \vec{G})^m$ (where n and m are integers), and we expand $(\hat{q} \cdot \hat{G})$ using the addition theorem,

$$(\hat{q} \cdot \hat{G}) = \cos\chi \cos\psi + \cos\phi' \sin\chi \sin\psi , \quad \text{(A12)}$$

where the angles [shown on Fig. 9(b)] are defined by

$$\cos\chi = \hat{q}_0 \cdot \hat{G} \quad \text{and} \quad \cos\psi = \hat{q}_0 \cdot \hat{q} . \quad \text{(A13)}$$

To first order in the small quantity q/k_F, the angles are given by

$$\cos\chi = G/2k_F \quad \text{and} \quad \cos\psi = p/q . \quad \text{(A14)}$$

With this information we discuss the two cases.

(i) *Even power of* $\vec{q} \cdot \vec{G}$. Only even powers of $\cos\phi'$ in the expansion of $(\vec{q} \cdot \vec{G})^m$ survive the ϕ' in-

tegration, which therefore [(A12)–(A14)] leaves a polynomial in p^2/q^2. The p integration is done by parts as in (A11) to leave a single integration over wave vector for resistivity. As an example we evaluate the double surface integral of $(\hat{q} \cdot \hat{G})^2$ as follows: From (A12) and (A14) we find

$$(1/2\pi) \int_0^{2\pi} d\phi' \, (\hat{q} \cdot \hat{G})^2 = \cos^2\chi \, p^2/q^2$$
$$+ \tfrac{1}{2} \sin^2\chi \, (1 - p^2/q^2) , \quad \text{(A15)}$$

and integrating by parts over p we have, for example,

$$\int_{-q_2}^{q_D} dp \int_{|p|}^{q_D} q \, dq \, (p^2/q^2) = \tfrac{1}{3} q_2^3 \int_{q_2}^{q_D} dq/q$$
$$+ \tfrac{1}{3} \left(\int_0^{q_D} + \int_0^{q_2} \right) q^2 \, dq . \quad \text{(A16)}$$

With (A14)–(A16) we write out the surface integrals of $S_T^{(0)}$ for the case in which phonon polarization vectors are purely transverse or longitudinal:

$$\int \int dS \, dS' [1 - (\hat{q} \cdot \hat{G})^2] \, (2 \sinh\tfrac{1}{2}\beta\hbar\omega)^{-2}$$

$$= (8\pi^2 k_F^2/G) \left[\tfrac{2}{3} \left(\int_0^{q_D} + \int_0^{q_2} \right) q^2 \, dq + (1 - \tfrac{1}{2}\sin^2\chi) q_2 \int_{q_2}^{q_D} q \, dq \; - \tfrac{1}{3}(\cos^2\chi - \tfrac{1}{2}\sin^2\chi) q_2^3 \int_{q_2}^{q_D} dq/q \right] (2 \sinh\tfrac{1}{2}\beta\hbar\omega)^{-2}$$

$$= (8\pi^2 k_F^2/G) \tfrac{4}{3} \int_0^{q_D} q^2 \, dq \, (2 \sinh\tfrac{1}{2}\beta\hbar\omega)^{-2} P_2(\Theta_2/T, \Theta_D/T) . \quad \text{(A17)}$$

One can see that the cutoff function P_2 is more complicated than in the text, where polarization directions were averaged over. The low-temperature value of $S_T^{(0)}$ remains unchanged, however.

The expression (A17) is proportional to T^3 at low-temperatures $T \ll \Theta_2$, so from (A1) $S_T^{(0)}$ is proportional to T^2. In general, an even power $(\vec{q} \cdot \vec{G})^{2l}$ in Π leads to a T^{2l+2} term in S (umklapp) at low temperatures.

(ii) *Odd powers of* $\vec{q} \cdot \vec{G}$. Each term in the expansion of an odd power of $\vec{q} \cdot \vec{G}$ must from (A12) be odd in either $\cos\phi'$ or $\cos\psi$. The terms which are odd in $\cos\phi'$ give vanishing angular integrals. The terms which are odd in $\cos\psi$ are also odd in p

to lowest nonvanishing order in q/k_F (A14), and therefore contribute to (A10) only for values of p greater than the threshold $2k_F - G$. The resulting temperature dependence falls exponentially for temperatures less than Θ_2, e.g., $\exp(-\Theta_2/T)$. The correction to $\cos\psi$, of order q/k_F, survives the p integration, but the resulting resistivity is suppressed by roughly a factor T/Θ_D over what one would otherwise expect. As a result, an odd power $(\vec{q} \cdot \vec{G})^{2l+1}$ in Π leads to a T^{2l+4} term in S at low temperatures. In particular $S^{(1)}$ is proportional to T^4.

For the sake of comparison these facts are collected in Table IV. We have written the leading term in each of the umklapp components of Π and S, ignoring all such details as phonon polarization effects and cutoffs Θ_2. In the low-temperature regime of interest in this paper, we would ordinarily retain only the lowest power of (T/Θ_D) in the calculations, $S^{(0)}$. However, $S^{(2)}$ must be kept as well in view of the differing prefactors, $V(G)$ being considerably smaller than $GV'(G)$, which is of order E_F. $S^{(1)}$ is ignored because of the extra factor of (T/Θ_D) discussed above, without which it would still be less than the sum $S^{(0)} + S^{(2)}$.

TABLE IV. Dominant terms in $\Pi^{(n)}$ and $S^{(n)}$, divided by $[GV'(G)]^2$.

n	$\Pi^{(n)}$	$S^{(n)}$
0	$G^4[V(G)/GV'(G)]^2$	$[V(G)/GV'(G)]^2 (T/\Theta_{DT})^2$
1	$qG^3V(G)/GV'(G)$	$V(G)/GV'(G) (T/\Theta_{DT})^4$
2	q^2G^2	$(T/\Theta_{DT})^4$
3	q^3G	$(T/\Theta_{DT})^6$
4	q^4	$(T/\Theta_{DT})^6$

*Work supported by the U. S. Office of Naval Research under Contract No. N00014-67-A-0077-0010, Technical Report No. 23.

[1]J. Garland and R. Bowers, Phys. Rev. Letters 21, 1007 (1968).

[2]J. W. Ekin, thesis (Cornell University, 1971), available from University Microfilms, Ann Arbor, Mich. (unpublished).

[3]I. A. Campbell, A. D. Caplin, and C. Rizutto, Phys. Rev. Letters 26, 239 (1971); A. D. Caplin and C. Rizutto, J. Phys. C 3, L117 (1970).

[4]W. E. Lawrence and J. W. Wilkins (unpublished); W. E. Lawrence, thesis (Cornell University, 1970), available from University Microfilms, Ann Arbor, Mich. (unpublished).

[5]J. M. Ziman, Electrons and Phonons (Oxford U.P., Oxford, 1960).

[6]The upper bound is equal to the true resistivity only when the trial distribution function satisfies the Boltzmann equation (1.8).

[7]This procedure is especially useful when the Fermi surface is distorted. The "remapping" restores continuity of the various Fermi-surface sheets.

[8]A. H. Wilson, Theory of Metals (Cambridge U.P., Cambridge, England, 1958), Appendix 5iii, p. 336.

[9]In the spirit of our two-plane-wave calculation, we use

form factors which fit Fermi-surface dimensions: for aluminum, N. W. Ashcroft, Phil. Mag. 8, 2005 (1963); and for indium, N. W. Ashcroft and W. E. Lawrence, Phys. Rev. 175, 938 (1968).

[10]We define the cutoff function P_2 in the approximation in which we average over polarization directions. The added complexity introduced into the cutoff formulas by assuming pure polarizations ($\lambda = L$ purely longitudinal and $\lambda = T$ purely transverse) is not warranted at temperatures near Θ_2 (2.16).

[11]Again the cutoff formula P_4 is defined for the average over polarization directions.

[12]In Al, $m_{opt}/m \approx \frac{5}{4}$ and in In the ratio is about $\frac{4}{3}$.

[13]D. L. Mills, Phys. Rev. Letters 26, 242 (1971); for discussion see D. Sherrington [Phys. Letters 35A, 399 (1971)] and B. G. Nickel and J. W. Wilkins [Phys. Rev. B 5, 5000 (1972)]. The large effect purported by the first paper is due to an error in analysis. See the latter two papers for a discussion of this point.

[14]J. W. Ekin and B. W. Maxfield, Phys. Rev. B 4, 4215 (1971); and D. Gugan (unpublished).

[15]E. Pytte, J. Phys. Chem. Solids 28, 93 (1967).

[16]J. G. Collins and J. M. Ziman [Proc. Roy. Soc. (London) 264A, 60 (1961)] use similar variables in their calculation of transport coefficients in the alkali metals.

Electronic Wave Functions in One-Dimensional Disordered Systems*

B. Y. Tong and T. C. Wong[†]

Department of Physics, University of Western Ontario, London, Ontario

(Received 14 July 1972)

The nature of wave functions in a one-dimensional disordered system is examined in terms of a model system in which the central portion of a cell is represented by the same potential in all cells and only the lengths of the flat arms vary randomly from cell to cell. It has been shown previously that although most wave functions are localized, states corresponding to the resonances states of the central potential have extended wave functions. Here we show that states close to these resonances also have fairly extended wave functions throughout the physical sample. Numerical calculations on a model system formed from symmetric square wells indicate that even in a highly disordered system there are wide energy ranges close to the resonances which have fairly extended wave functions. Wave functions having energies in the allowed bands of the corresponding periodic lattice are also weakly localized, but their degree of localization is raised as a whole with an increase in disorder, whereas an increase in disorder only narrows the energy range of these fairly extended states.

I. INTRODUCTION

Extensive reviews on the electronic properties of one-dimensional disordered systems are available.[1-9] Owing to the complexity of the solutions and their interpretation, and because of the recent indications of the experimentally measurable physical systems,[10,11] the one-dimensional disordered systems are still being actively studied.[12-47] The two key questions studied in the electronic properties of such systems are (a) the existence of energy gaps and the density of states,[12-25,41-44] and (b) the

localization of electronic wave functions.[26-40,46]

We studied the problems using the phase-transfer method.[2,41-48] A wave function connecting through a cell of a potential shown in Fig. 1 is represented by a phase-transfer matrix M:

$$\psi_{\text{left}} = A(x)e^{ikx} + B(x)e^{-ikx} , \tag{1}$$

$$\psi_{\text{right}} = A'(x)e^{ikx} + B'(x)e^{-ikx} , \tag{2}$$

$$\begin{pmatrix} A \\ B \end{pmatrix} = M \begin{pmatrix} A' \\ B' \end{pmatrix} ,$$

where